Structure and self-assembly of fullerene-containing molecular systems

VASILY T. LEBEDEV[a*], YULY S. GRUSHKO[a], GYULA TÖRÖK[b]
[a]*Petersburg Nuclear Physics Institute, NRC Kurchatov Instutute, 188300 Gatchina, Leningrad distr., Russia*
[b]*Wigner Research Centre of HAS, Research Institute for Solid State Physics and Optics, Budapest, POB-49, Hungary*

Hydroxylated fullerenes $Gd@C_{82}(OH)_X$ (x ~ 20) with Gd atoms inside carbon cages have been studied by small-angle neutron scattering in light water by the variation of pH = 4-7 via salts' addition in order to understand the characters of structural transitions and the ways of fullerenols' supramolecular structures control and regulation. As it was found, the globular (droplet-like, diameter ~ 50 nm) clusters of fullerenols in pure water (pH = 4-5) become instable when the salts introduced into solutions (pH = 7) cause the formation of fullerenols' chain-like aggregates (correlation radius ~ 20 nm) the structure of which is dependent on the type of salt.

(Received November 12, 2012; accepted April 11, 2013)

Keywords: Fullerenes, Small angle neutron scattering, Structure, Solutions

1. Introduction

Synthesis of endohedral metallofullerenes, following separation and purification [1-5] makes possible their advanced applications in biology and medicine to produce new effective contrasting agents (MRI-diagnostics), radioactive isotopic tracers, pharmaceutical preparations [6-10].

These prospects are closely related to the problem of transfer of insoluble fullerenes into aqueous (physiological) media. This problem can be solved by the development of the methods (hydroxylation, grafting water-soluble oligomers, polymers) for producing the hydrophilic derivatives of fullerenes [2-4,8,9,11,12].

However, the water-soluble fullerenes demonstrate various assembly phenomena under the influence of numerous factors (concentrations of fullerenes, additives, pH, temperature) [13-15]. The related features of fullerrenols' ordering in solutions remain not yet studied systematically. Meanwhile, the examination of fullerenols' behavior in solutions is of fundamental and practical interest assuming the opportunities of fine regulation of their functional properties (e.g. MRI-contrast via enhancement of surrounding protons' spin relaxation rate) being strongly dependent on fullerenols' arrangement in molecular clusters possessing a lot of parameters (size, mass, anisotropy and porosity).

The aggregates of fullerenols (water-soluble derivatives) in solutions have been observed by light, X-ray and neutron scattering in the range 10^0 - 10^3 nm [13,15-17]. Since the molecular mechanisms of self-assembly are still not decoded, the extended study seems to be necessary. The aim of work is the research of molecular ordering of fullerenols $Gd@C_{82}(OH)_X$ (x ~ 20) in light water as determined by the chemical type and content of additives in solutions.

2. Experimental

Small-angle neutron scattering experiments (SANS) on the solutions of fullerenols have been carried out (diffractometer "Yellow submarine", wavelengths λ = 0.751; 0.386 nm, RISSPO, Budapest) in the range of momentum transfer q = 0.08-4.5 nm^{-1} to observe the molecular structures at scales $R \sim 2\pi/q \sim 10^0$-10^2 nm. In aqueous (H_2O) solutions the concentration of fullerenols was kept constant, C = 0.3 g/dl. The series of the samples 1-3 has included the binary solution of $Gd@C_{82}(OH)_X$ (x ~ 20) (scheme below) and ternary systems prepared by the addition of sodium citrate or phosphate (Table 1).

3. Results and discussion

3.1 Small-angle Neutron Scattering

The neutron scattering intensities $I_S(q)$ for the samples (25°C, layer thickness d_S = 1 mm) have been normalized to the data $I_W(q)$ for light water (layer thickness d_W = 1 mm) at the same conditions measured. The differential cross sections of solutions (per unit solid angle Ω, and cm^3) are evaluated in absolute units, $d\sigma/d\Omega = (I_S/I_W)(d_W/d_S)d\sigma_W/d\Omega$. Here $d\sigma_W/d\Omega$ is the cross section of H_2O (per cm^3) served as a standard [18]. The samples are chosen relatively thin (d_S = 1 mm) to prevent a multiple coherent scattering.

Their transmissions Tr ~ 0.5-0.6 indicate mainly the extinction due to the incoherent scattering from light water, while the coherent one contributes only ~ 1 %.

The cross sections of solutions (notation $\sigma(q) = d\sigma/d\Omega$) demonstrate the increase at low $q \leq 1$ nm^{-1} from the level of incoherent background $B \approx 0.8$ cm^{-1} (Fig.1). It reflects a substantial clustering of fullerenols at scales $R \sim 2\pi/q$ being much larger than molecular diameter ~1 nm.

Table 1. Composition of the samples, pH values

N	Fullerenes Content, g/dl	Salt Concentration, g/dl		pH
		Cintrate	Phosphate	
1	0.3	-	-	4-5
2	0.3	1.4	-	7
3	0.3	-	0.44	7

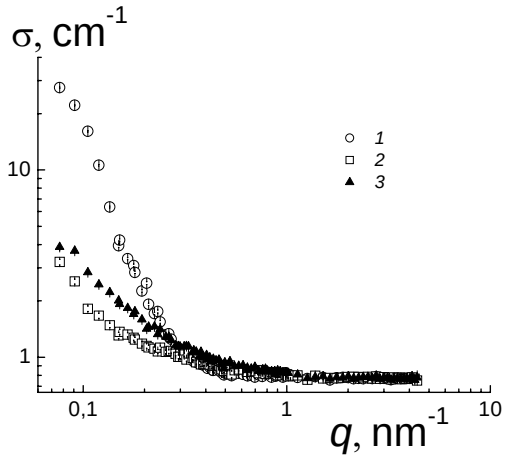

Fig. 1. Cross section of fullerenols' in H_2O: 1 – data for binary solution of $Gd@C_{82}(OH)_X$; 2, 3 – data for ternary solutions with citrates and phosphates.

It is clear (Fig.1), the addition of salts leads to the weakening of scattering by an order in magnitude at $q \leq 1$ nm^{-1}. The salts stimulate the dissolution of visible molecular clusters. At the same time, the transmission becomes smaller, i.e. the scattering outside the central cell of detector is enhanced and/or concentrated at very low $q < q_{min} = 0.08$ nm^{-1}. The transmission deficit for citrate solution, ΔTr ~ -1 %, is much smaller than that in system with phosphate, ΔTr ~ -10 %. This indicates a strong action of phosphate as a structuring agent.

The transformation of solutions' structure includes not only the changes of clusters' amount and dimensions, but also a change of their geometry. This is evident from the data analysis at relatively high q = 0.2-4.5 nm^{-1} when the cross sections obey the function

$$\sigma(q) = J/q^{Df} + B . \qquad (1)$$

Here J is the coefficient characterizing the scattering ability of observed objects. The parameter D_f describes their geometry (fractal dimension) (Tab.2). The data approximation with the function (1) allowed separate incoherent background and extract the coherent part $\Sigma(q) = [\sigma(q)-B]$ described by the function J/q^{Df} (Fig.2). In the binary solution of fullerenols the exponent $3 < D_f < 4$ indicates the globular particles with imperfect borders. Their surface has the fractal dimension $D_S = 6 - D_f \approx 2.3 > 2$.

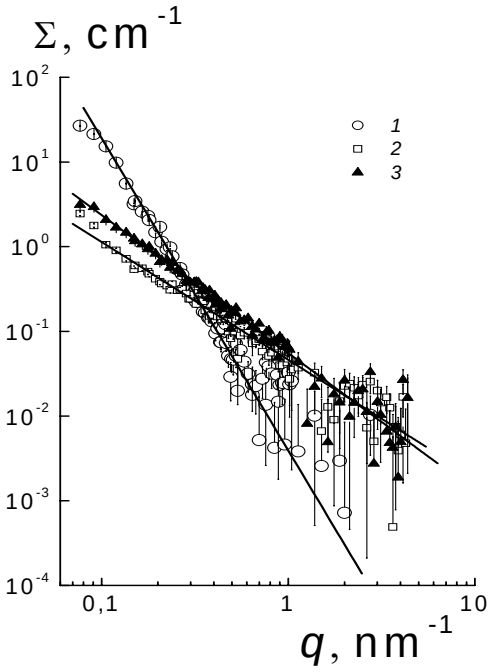

Fig.2. Data approximation with the function (1), the coherent cross section is presented.

Table 2. Parameters of function (1): coefficient J, fractal dimension of clusters D_f, incoherent background B.

N	$J \cdot 10^2$, cm^{-1}nm^{-D}	D_f	B, cm^{-1}
1	0.44 ±0.03	3.63 ±0.05	0.770 ±0.001
2	4.62 ±0.30	1.39 ±0.05	0.762 ±0.002
3	5.55 ±0.28	1.63 ±0.05	0.763 ±0.002

On the other hand, in salt solutions the fullerenols create chain-like structures of low density. The addition of citrate makes the parameter $D_f \approx 1.4 < D_F = 5/3$ even smaller than Flory exponent D_F for flexible polymers with excluded volume in good solution. In chain aggregates, the units repulse each other, and resulting stretching of chains is evident from low $D_f \approx 1.4$. However, in systems with phosphate where $D_f \approx D_F$, the chains take conformation like this one for polymer coil with excluded volume in good solvent.

3.2 Molecular correlations

The dependence (1) testifies the observed clusters as the sequences of stiff fragments (rod-like units, length L_P, cross section area S_t) the mutual correlations of which are defined by the exponent D_f. If the origin of coordinates (R=0) is fixed at a unit, the chain fragment captured inside

the sphere (radius R) has the volume $V_R = (2L_PS_t)(R/L_P)^{Df}$. In the spherical layer (radius R, thickness dR) the occupied volume $dV_R = (dV_R/dR)dR = (2D_fS_t/L_P^{Df-1})R^{Df-1}dR$ is proportional to the probability to find a chain unit at the distance R from the centre. Thus, the pair correlation function of units is expressed by $\gamma_o(R) = (D_fS_t/2\pi L_P^{Df-1})R^{Df-3}$. The Fourier-transform of $\gamma_o(R)$ gives the scattering cross section [19, 20] for such fractal objects' ensemble

$$\sigma(q)=4\pi(\Delta K)^2\varphi\int\gamma_o(R)[\sin(qR)/(qR)]R^2dR = J/q^{Df}, \quad (2)$$

$$J(L_P) = 2S_t(\Delta K)^2\varphi D_f\Phi(D_f)/L_P^{Df-1}.$$

Here ΔK is the contrast factor for chains, φ is their volume fraction in solution. The coefficient $J(L_P)$ as a function of length L_P includes also known parameters ΔK, D_f, the integral $\Phi(D_f) = \int X^{Df-2}\sin X dX \sim 1$ in the limits $(0,\infty)$. The chain cross section area S_t was found from the data modified by the factor q^{Df} (Fig.3).

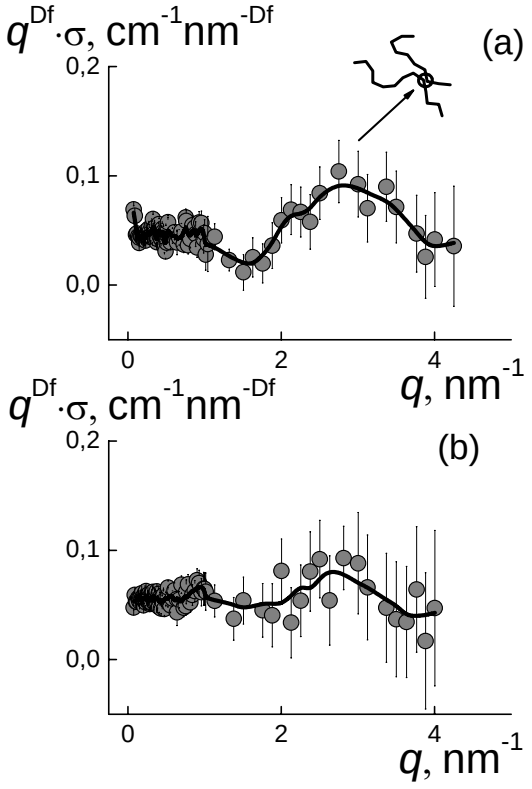

Fig. 3. Modified cross sections $q^{Df}\sigma(q)$ for solutions with citrate and phosphate (a,b). Lines are spline-functions.

The modified cross sections $q^{Df}\sigma(q)$ exhibit the peaks (Fig.3). Their maxima positions $q^* = 2.75$ nm^{-1}, $q^* = 2.63$ nm^{-1} (samples 2, 3) results from the interference of neutron waves scattered from the chains in contact at minimal distance $d_U \approx 7.725/q^*$ (chain diameter). Here the value of q* corresponds to the maximum of Debye function $\sin(qd_U)/(qd_U)$. The following chain diameters $d_U = 2.8 \pm 0.1$ nm, $d_U = 2.9 \pm 0.1$ nm are still bigger by the factor ~ 2.5 than Gd@C_{82} diameter $d_F \approx 1.12$ nm [1]. Hence, the observed structures are the bunches of elementary filaments of fullerenols (diameter ~ d_F). For the samples 2 and 3, the numbers of filaments

$$n_C = 4.0 \pm 0.3, \quad n_C = 4.4 \pm 0.3$$

were evaluated from chains' cross sections $S_t = \alpha\pi d_U^2/4$ taking into account the part of area $\alpha \approx 0.9$ (dense package of cylinders) occupied by fullerenols. Each molecule Gd@$C_{82}(OH)_X$ has the cross section area $S_F = \pi d_{EF}^2/4$ where fullerenol's diameter $d_{EF} = 2r_{EF} \approx 1.33$ nm is defined by its effective radius $r_{EF} \approx 0.667$ nm increased due to attached OH-groups as compared to known fullerene radius $r_F = d_F/2 = 0.56$ nm. Finally, it gives the cross section area $S_{EF} = \pi r_{EF}^2 = 1.40$ nm^2 and the volume of fullerenol $V_{EF} = 1.24$ nm^3. At last, the length of unit is estimated, $L_P = 5.2 \pm 1.4$ nm and $L_P = 3.1 \pm 0.4$ nm for the samples 2, 3.

The transition from citrate to phosphate solution (keeping pH = 7) makes the local flexibility of chains higher, and reduce their persistence length ~ $L_P \approx 5.2$ nm → 3.1 nm almost to the diameter of chain $L_P \sim d_U$. Moreover, the correlations of units are weakened also. So the stretched chains undergo a transformation into the coils being similar to polymer chain with excluded volume in good solvent. In salt solutions an aggregate of fullerenols looks like a cylindrical micelle of surfactant. This reflects a common nature of hydrophobic and hydrophilic interactions governing molecular self-assembly, although the difference in behaviors of fullerenols and ordinary surfactants in solutions arises from a quasi-spherical shape of fullerenoles with hydrophobic nuclei and hydrophilic shells in contrast to rod-like surfactant molecules. A quasi-spherical fullerenol may be considered as an analog of spherical micelle of surfactant. However, in micelles a nano-phase separation is a result of molecular stacking, while in the case of fullerenols it is preset chemically. The chain-like formations of fullerenols represent a higher level of structuring where fullerenols play a role of effective micelles associated in solution. Presently, any other similar cylindrical assemblies of micelles are not found.

The specific geometry defines the dimensions of fullerenols' structures evaluated from the data transformation into the spectra $G(R) = R^2\gamma(R)$ where

$$\gamma(R) = (\Delta KV_1)^2 < \Delta n(0)\Delta n(R) > =$$

$$= (1/2\pi)^3\int\sigma(q)[\sin(qR)/(qR)]4\pi q^2dq \quad (3)$$

The correlation function $\gamma(R)$ includes the volume of a molecule V_1 and the deviations $\Delta n(0)$, $\Delta n(R)$ of molecular concentrations from the average level in the points separated by distance R. The isotropic correlations in spherical layers are described by the functions $G(R)$ (Fig.4). The quality of description of the data by the spectra $G(R)$ is evident from the fit of cross sections with the related scattering functions (Fig. 5).

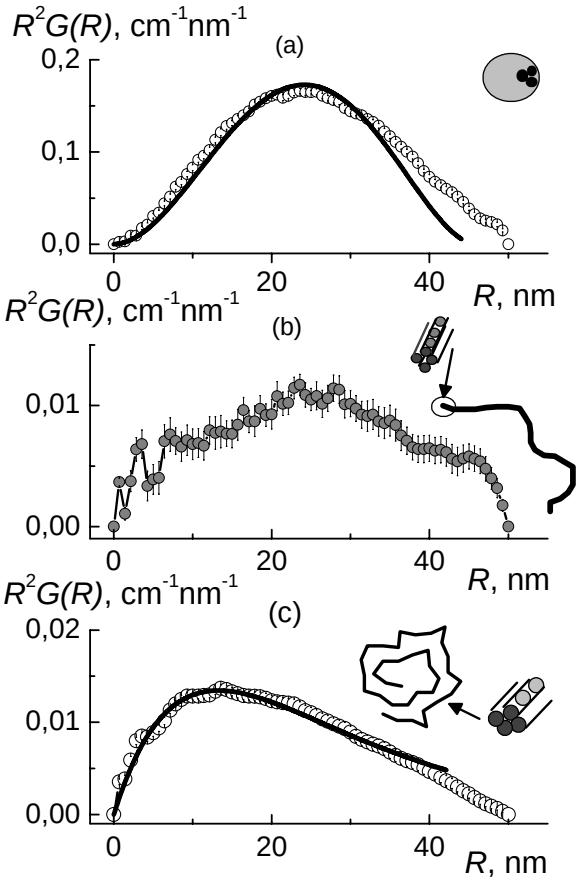

Fig. 4. Correlation functions G(R) vs. radius R for pure fullerenol solution (a), systems with citrate (b) and phosphate (c). Lines (a, c) are fitting functions (4,5).

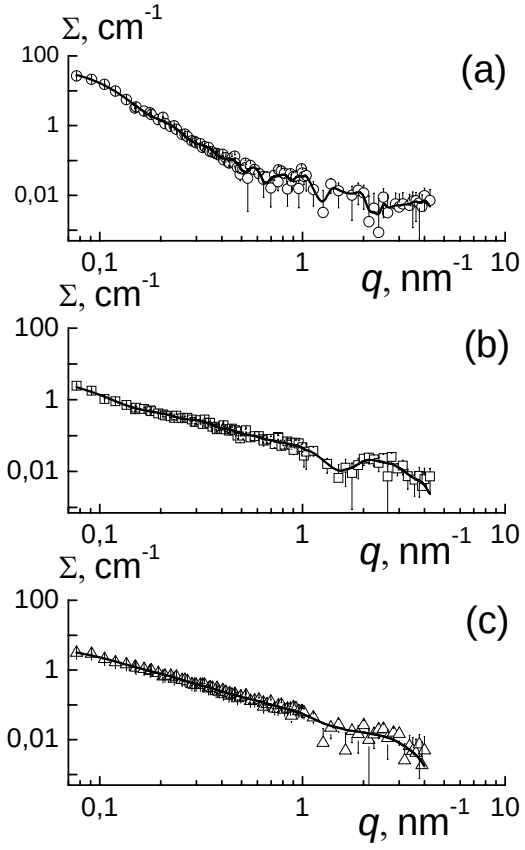

Fig. 5. Cross sections of fullerenols' solution (a), and ternary systems containing citrate (b)or phosphate (c). Lines are the scattering functions corresponding to G(R) (Fig.4).

The behavior of $G(R)$ in the range R = 0-50 nm undergoes a qualitative altering due to salts' addition. For binary system (Fig.4a), the profile of $G(R)$ is quite symmetric regarding to maximum position. In the first approximation it is described by the function for sphere

$$G(R) = A_S \cdot R^2[1 - (3/4)(R/R_S) + (1/16)(R/R_S)^3] \qquad (4)$$

The parameter $A_S = (1.04 \pm 0.1)\cdot 10^{-3}$ cm^{-1}nm^{-3} reflects the scattering ability of molecular aggregates having in average the radius $R_S = 23.0 \pm 0.1$ nm. The spread of their size from the R_S leads to a deviation of spectrum from the function (4) at $R \geq 30$ nm.

On the other hand, the profile $G(R)$ for system with phosphate (Fig.4c) is asymmetric and adheres the function

$$G(R) = A_C R \cdot \exp(-R/R_C) \qquad (5)$$

for gaussian polymer coil (fractal dimension $D_f = 2$) with correlation radius R_C. The coefficient $A_C = (2.76 \pm 0.03)\cdot 10^{-3}$ cm^{-1}nm^{-2} depends on contrast factor, fullerenols' content, clusters' masses. Since the magnitude of the exponent obtained above $D_f < 2$, the gaussian model is applied in the first approximation only.

In frames of this model the $R_C = 13.2 \pm 0.1$ nm gives the estimate of chain gyration radius $R_G = \sqrt{3}\, R_C = 22.9 \pm 0.2$ nm. It is greater by ~ 30 % than the size of spherical cluster of pure fullerenols, $R_{GF} = R_S(3/5)^{1/2} = 17.8 \pm 0.1$ nm. Hence, the binary solution is ordered more compactly than the ternary system with phosphate.

As compared to the system with phosphate, in solution with citrate the profile of $G(R)$ looks like a plateau with hump (Fig.4b). Such correlations, $G(R) \approx$ const in a wide spatial range, testify some objects like thin rods. In the interval $0 \leq R \leq 50$ nm the behavior of $G(R)$ (Fig.4b) confirms a stretched geometry of fullerenols' chains (radius R~20-30 nm) composed of units of length L_P ~5 nm. The correlations within a unit are revealed as a peak in the interval R = 0-5 nm where maximum at R^* ~ 3 nm ~ $L_P/2$ corresponds to a half of unit's length.

More precisely clusters' dimensions and aggregation numbers were found from the integrals over spectra $G(R)$. The forward cross section of solution $\sigma(q\to 0) = \sigma_o = 4\pi S_1 = (\Delta K)^2 \varphi V_C$ is defined by the integral $S_1 = \int G(R)dR$. Its evaluation gives the dry volume of cluster $V_C = \sigma_o/(\Delta K)^2\varphi$ and the aggregation number $N_C = V_C/V_{EF}$ (Tab.3). From the integrals the gyration radii were obtained also (Tab.3)

Table 3. Cross sections of solution σ_o, aggregation numbers N_C, gyration radii of clusters R_G

N	σ_o, см$^{-1}$	$N_C \cdot 10^{-3}$	R_G, нм
1	59.9 ±0.2	11.1 ±0.1	19.1 ±0.1
2	4.66 ±0.08	0.87 ±0.02	19.3 ±0.3
3	5.24 ±0.04	1.21 ±0.01	16.4 ±0.2

The obtained parameters (Tab.3) testify an intense aggregation in binary system, $N_C \sim 10^4$. While the salt addition depresses it, and the number of molecules in cluster $N_C \sim 10^3$ becomes lower by an order in magnitude. Although the radius of cluster R_G remains still unchanged in the presence of citrate, the addition of phosphate causes the decrease of cluster dimension by ~ 10 %. As a result, in salt solutions the clusters are rarefied by factor ~ 10.

The concentrations of fullerenols inside clusters differ strongly from each other: $N_m = N_C/(4\pi/3)R_G^3 \approx 4 \cdot 10^{20}$ cm^{-3}, $3 \cdot 10^{19}$ cm^{-3} and $7 \cdot 10^{19}$ cm^{-3} for binary and ternary solutions (citrate, phosphate). Such local densities surpass by 1-2 orders in magnitude the average molecular concentration $1.25 \cdot 10^{18}$ cm^{-3} in the samples. In binary system the fullerenols fill ~ 50 % of the volume of aggregates like droplets with diameter ~ $2R_G(5/3)^{1/2}$ ~50 nm. However, in salt solutions fullerenols occupy only ~4% or ~8 % of the volume of aggregates rarefied. These entities are ~10 times more numerous than dense formations in binary solution.

These results give the detailed information on the behaviors of fullerenols in solutions and subtle features of their clustering. The latter should be discussed as compared to fullerenes C_{60} solutions treated theoretically [21] as a specific "cluster state" of matter. Usually the clustering of C_{60} can be observed in aromatic solvents, e.g. in benzene, by dynamic light scattering [22]. SANS-studies of C_{60} in toluene [23] carried out for saturated solutions in quasi-equilibrium state (20°C, stored during one year) detected some large-scale structures ($\geq 10^2$ nm, fractal dimension $D_f \approx 2.9$) composed of droplet-like clusters (correlation radius $R_C \sim 3$ nm, aggregation number ~ 50) predicted by thermodynamic theory [21]. Also in other solvent (CS_2) the small-sized C_{60} clusters (aggregation numbers < 10) have been found by SANS [24,25].

During the last decade, the fundamental and practical efforts are attracted to the problem of transfer of fullerenes C_{60} into aqueous media. For example, it can be done by a change of solvent (ultrasonic treatment of mixtures of water and fullerene solution in benzene, toluene). Aromatic solvent evaporation gives the stable dispersions of fullerenes in water via formation of globular clusters (droplet-like, size ~ 100 nm, smooth surface) studied by SANS [26].

The water-soluble endohedral fullerenes derivatives, $Gd@C_{60}[C(COOH)_2]$ and $Gd@C_{60}(OH)_X$, have been synthesized and examined in solutions as potential MRI contrast agents being sensitive to the aggregation modifying their functional properties [27]. In aqueous medium these molecules showed an association into clusters (~30-90 nm) [27]. In following study [28] fullerenols $Gd@C_{60}(OH)_X$ were investigated as pH-responsive MRI contrast agents: at low pH the Gd-containing molecular clusters become larger and provide a high relaxivity.

In our recent work [17], the fullerenols $C_{60}(OH)_X$ in aqueous solutions (25°C, pH = 5-8) have been studied by SANS. The system with $C_{60}(OH)_X$ (X ~ 20, content C_F = 0.5 mg/ml, pH = 5) displayed a stronger short range order by the increase of pH → 8 due to Na-citrates' addition. At the same time, the Na-phosphates have induced the formation of two-level structures: tiny particles (size ~ 6 nm) packed into large clusters (gyration radius ~ 30 nm). These peculiarities of fullerenols' association concerned only globular clusters. Any other structures (chain-like, branched) are not detected. The previous SANS-study [16] of hydroxylated fullerenes $Gd@C_{82}(OH)_X$ in water showed also molecular clustering at scale ~20-30 nm. At pH increasing from 4-5 to 7-8 it was detected a transition from dense branched structures (fractal dimension $D \sim 2.5$) to rare coil-like objects ($D \sim 1.6$). These data together with the obtained above results clarify the nature of fullerenols' association into different structures.

4. Conclusion

The observed enhancement of fullerenols' solubility and transition from globular to chain-like structures by salts' addition can be treated as a result of formation of hydrogen bonds between fullerenols and acid groups creating a shell around fullerenols by hydration. The shells stabilize stretched conformations of chain-like structures via fastening rigidity, increasing persistence length. Together with hydrogen bonds the dipole interactions (electric, magnetic) between fullerenols in chain structures and dipole forces between them and associated acid groups are considered as responsible for chain-like structures formation.

The study of structural transformation in fullerenols' solutions enabled us to establish the crucial features of their association. Except of fundamental importance, this is useful in order to find some effective ways to form a desirable morphology of hydroxylated endometallofullerenes in aqueous media for biomedical and technical applications.

Acknowledgements

The work is supported by RFBR (grant 12-03-120-20-ofi_m).

Authors acknowledge V.P. Sedov, V.A.Shilin, V.S. Kozlov,V.V. Kukorenko, S.G. Koleslik, I.N. Ivanova for the samples preparation and the help in data treatment.

This paper contains results presented at the International Summer School and Workshop "Complex and Magnetic Soft Matter Systems: Physico-Mechanical Properties and Structure", CMSMS 12, 3-7 September 2012, Alushta, Ukraine (http://cmsms.jinr.ru/).

References

[1] H. Shinohara, Rep. Prog. Phys. **63**, 843 (2000).

[2] H. Kato, K. Suenaga, M. Mikawa, M. Okumura, N.Miwa, A.Yashiro, H.Fujimura, A. Mizuno, Y. Nishida, K. Kobayashi, H. Shinohara, Chem. Phys. Lett. **324**, 255(2000).

[3] C.Y.Shu, L.H. Gan, C.R. Wang, X. Pei, H. Han, Carbon. **44**, 496 (2005).

[4] M.D. Diener, J.M. Alford, S.J. Kennel, S. Mirzadeh. J. Am. Chem. Soc. **129**, 5131 (2007).

[5] J.W. Raebiger, R.D. Bolskar, J. Phys. Chem C. **112** 7), 6605 (2008).

[6] D.W.Cagle, J.M.Alford, J.Tien, L.J.Wilson, Gadolinium-Containing fullerenes for MRI contrast agent application. In Fullerenes: Recent Advances in the Chemistry and Physics of fullerenes and Related Materials. Kadish K., Ruoff R. The Electrochemical Society, Inc.: Pennington, NJ, **4,** 361-368 (1997).

[7] L.J. Wilson, Interfase. **8,** 24 (1999).

[8] C. Shu, C.-R.Wang, J.-F. Zhang, H. W. Gibson, H. C. Dorn, F. D. Corwin, P. P. Fatouros, T.J.S.Dennis, *Chem. Mater.* ***20,*** 2106 (2008).

[9] Y. Zhao M.J. Heben, A.C. Dillon, L.J. Simpson, J.L. Blackburn, H. C. Dorn, H.W.Gibson, P.P. Fatouros, Ch.-R. Wang, X.-H. Fang, Bioconjugate Chem. **19**, 651(2008).

[10] D. K. MacFarland , K. L.Walker, R. P. Lenk, S. R. Wilson, K. Kumar, C. L. Kepley, J. R. Garbow, J. Med Chem. **51**(13), 3681(2008).

[11] V. Lebedev, Gy. Torok, L. Cser, A. Len, D.Orlova, V. Zgonnik, E. Melenevskaya, L. Vinogradova, W. Treimer, J.Appl.Cryst**. 36,** 646(2003).

[12] V.T. Lebedev, Gy.Torok, E.Yu. Melenevskaya, L.V.Vinogradova, I.N. Ivanova, Fullerenes, Nanotubes and Carbon Nanostructures. **16**(5-6), 603(2008).

[13] B. Sitharaman, R.D. Bolskar, I. Rusakova, L.J. Wilson, Nano Lett. **4**, 2373(2004).

[14] E. Toth, R.D. Bolskar, A. Borel, G. Gonzalez, L. Helm, A.E. Merbach, B. Sitharaman, L.J. Wilson, J. Am. Chem. Soc. **127,** 799 (2005).

[15] S. Laus, B. Sitharaman, E.Toth, R.D. Bolskar, L. Helm, S. Asokan, M.S. Wong, L.J. Wilson, A.E. Merbach. J. Am. Chem Soc.**127**, 9368(2005).

[16] V.T. Lebedev, Yu.S.Grushko, D.N. Orlova, V.S. Kozlov, V.P. Sedov, S.G. Kolesnik, V.V. Shamanin, E.Yu. Melenevskaya, Fullerenes, Nanotubes and Carbon Nanostructures, **18** (4), 422 (2010).

[17] I. V. Nikolaev, V. T. Lebedev, Yu. S. Grushko, V. P. Sedov, V. A. Shilin, Gy. Török, E. Yu. Melenevskaya, Fullerenes, Nanotubes, and Carbon Nanostructures. **20** (4-7), 345 (2012).

[18] P. Lindner, J. Appl. Cryst. **33**, 807 (2000).

[19] D. I. Svergun, L. A. Feigin, X-ray and neutron small-angle scattering. Moscow: Nauka. 1986. 279 P.

[20] D. I. Svergun, J. Cryst. **25**, 495(1992).

[21] V. N., Bezmel'nitsyn, A. V., Eletskii, M. V. Okun', Usp. Fiz. Nauk. **168**(11), 1195 (1998).

[22] S. Nath, H.Pal, A.V. Sapre, Chem. Phys. Lett. **327**, 143 (2000).

[23] Gy.Torok, V.T. Lebedev, L. Cser, Physics of the Solid State **44** (3), 572 (2002).

[24] Yu. B., Melnichenko, G. D.Wignal, R. N. Compton, G. Bakale, J. Chem. Phys. **111**, 4724 (1999).

[25] T. V. Tropin, M. V. Avdeev, V. L. Aksenov, Fullerenes, Nanotubes, Carbon Nanostructures. **16,** 616 (2008).

[26] A.O. Khokhraykov, M.V.Avdeev, V.L.Aksenov, L.A. Bulavin, J. Mol. Liq. **127**, 73 (2006).

[27] B.Sitharaman, R.D.Bolskar, I. Rusakova, L.J. Wilson, Nano Lett. **4**, 2373 (2004).

[28] E.Toth, R.D.Bolskar, A.Borel, G.Gonzalez, L.Helm, A. E. Merbach, B. Sitharaman, L. J. Wilson, J. Am. Chem. Soc. **127**, 799 (2005).

*Corresponding author: vlebedev@pnpi.spb.ru